
Table-Based Neural Units: Fully Quantizing Networks for Multiply-Free Inference

Michele Covell¹ David Marwood¹ Shumeet Baluja¹ Nick Johnston¹

Abstract

In this work, we propose to quantize all parts of standard classification networks and replace the activation-weight-multiply step with a simple table-based lookup. This approach results in networks that are free of floating-point operations and free of multiplications, suitable for direct FPGA and ASIC implementations. It also provides us with two simple measures of per-layer and network-wide compactness as well as insight into the distribution characteristics of activation-output and weight values. We run controlled studies across different quantization schemes, both fixed and adaptive and, within the set of adaptive approaches, both parametric and model-free. We implement our approach to quantization with minimal, localized changes to the training process, allowing us to benefit from advances in training continuous-valued network architectures. We apply our approach successfully to AlexNet, ResNet, and MobileNet. We show results that are within 1.6% of the reported, non-quantized performance on MobileNet using only 40 entries in our table. This performance gap narrows to zero when we allow tables with 320 entries. Our results give the best accuracies among multiply-free networks.

1. Introduction to Network Quantization

Deep neural networks are being employed in an ever-growing number of applications. Though these networks are often trained on computers with powerful GPUs, inference is increasingly happening on end-user devices. To address the enormous range of memory, bandwidth, and computation constraints that must be handled for successful wide deployment of neural-network-based applications, there has been renewed interest in efficient inference. One promising technique is network quantization. Research into neural-network quantization is not new; it has spanned decades and

included numerous approaches (Balzer et al., 1991; Marchesi et al., 1993; Yi et al., 2008; Vanhoucke et al., 2011; Anwar et al., 2015; Courbariaux et al., 2016; Han et al., 2016; Hubara et al., 2016; Zhou et al., 2016; Garland & Gregg, 2017; Deng et al., 2017; Wu et al., 2018; Baluja et al., 2018). (Guo, 2018) provides an excellent survey of the prior work in this area. His analysis includes a useful characterization of the methods as using either fixed or adaptive codebooks for the weight quantization. In this paper, we introduce new adaptive (Section 3.3) and new fixed (Section 3.4) quantization approaches.

There is little agreement on what it means to quantize a network. For example, (Courbariaux et al., 2016; Li et al., 2017) quantize only the weights but not the biases or the activations, while (Cai et al., 2017) focuses on activations. Recent efforts, including (Zhou et al., 2016; Deng et al., 2017), quantized *some* of the weights and *some* of the activations but not all of them. Some studies quantize the network uniformly to allow operations using fixed-point arithmetic (Jacob et al., 2018), others quantize each channel of each layer independently (Krishnamoorthi, 2018). Successful previous studies have employed varying levels of discretization, ranging from bi-level and tri-level weights to 4- and 8-bit instantiations. Some use adaptive quantization (Gong et al., 2014; Choi et al., 2017; Achterhold et al., 2018) and others use fixed codebooks (Tang & Kwan, 1993; Hwang & Sung, 2014; Kim et al., 2014; Courbariaux et al., 2015; Zhu et al., 2016). Finally, as expected, the degree of change needed in the training algorithms varies significantly (Rastegari et al., 2016; Zhou et al., 2016; Tang et al., 2017; Zhou et al., 2017).

This range of definitions for what it means to quantize a network makes it difficult to compare approaches. In this study, as in (Baluja et al., 2018), we start with the premise that we should be able to quantize *all* parts of the network: the biases, the weights, and the activations. Full quantization allows us to avoid all floating-point operations and even fixed-point multiplication, replacing it with a Look-Up-Table (LUT). For an FPGA implementation, there is a reasonably direct trade-off between the expense of floating point and the memory needed for our LUTs: if the LUT size is less than a few thousand entries, it takes fewer FPGA re-

¹Google Research, Mountain View, CA, USA. Correspondence to: Michele Covell <covell@google.com>.

sources than a CLB-based floating-point multiply (Marcus, 2004).

Full quantization also allows us to develop two usable measures with which to compare quantizations, *neural-unit complexity (NUC)* and *network-wide non-compactness (NWNC)*. Inspired by (Chatterjee, 2018), which used LUTs in the study of network generalization and capacity, we reformulate the standard multiplication of activations and weights as a simple table-cell look-up. The sizes of the required LUTs give a partial measure of complexity and compactness: with NUC, we use the per-layer LUT size as a local measure of complexity and, with NWNC, we use the combined LUT sizes across the full network as a measure of the (non-)compactness of the full representation. With these measures, we are able to compare adaptive codebooks to fixed ones, to examine the best allocation between the activation and weight quantization levels, and to examine the gain in NWNC of using a single global set of weight quantizations compared to layer-specific weight quantizations.

To avoid moving unnecessarily far from the underlying floating-point networks that we are analyzing, we propose two simple, highly localized changes to standard deep-learning training regimes. Though simple, these yield fully discretized networks with minimal accuracy loss; these are described in Section 2. In Section 3, we examine four alternative weight-quantization approaches, using AlexNet (Krizhevsky et al., 2012) as our target. In Section 4, we examine two approaches to activation quantization: uniform linear and *octave sampling*. Using octave sampling for both weights and activations, we are able to move away from doubly indexed LUTs to much smaller single-index tables. In Section 5, we conduct extensive empirical tests, comparing our results to others on three different-sized networks: AlexNet, for comparison with (Wu et al., 2018; Zhou et al., 2016; Hubara et al., 2016; Rastegari et al., 2016; Lin et al., 2015)); ResNet-101, for a large-network study; and MobileNet, for networks targeted at mobile devices. Finally, conclusions are presented in Section 6.

2. LUT-based Networks

In this section, we present the quantization procedure, originally described in (Baluja et al., 2018). We quantize every portion of the network: all weights (including biases) and activations. For ease in exposition, we begin with the process of inference used in our quantized LUT-based networks. Then we return to training.

2.1. Inference using LUT-based Networks

To eliminate *all* multiplications and *all* floating-point operations, (Baluja et al., 2018) used doubly-indexed LUTs that hold the product of all the quantized weights and activa-

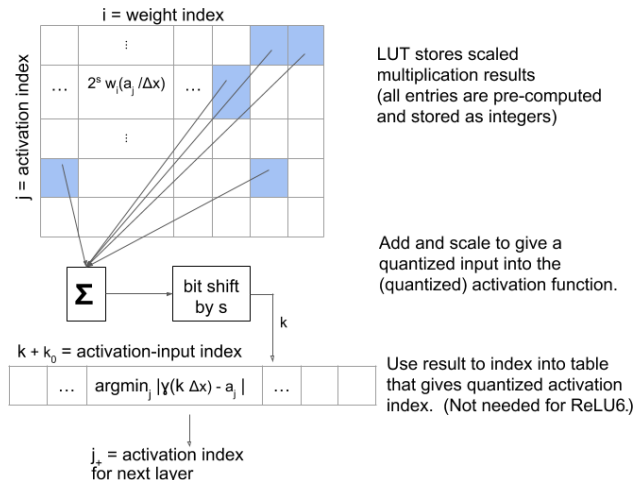


Figure 1. LUT-based neural unit. $LUT(i, j) = \frac{2^s}{\Delta x} w_i a_j$ (for quantized weight w_i and quantized activation-output a_j) replaces *all* multiplies at inference time. These values are summed to give $2^s \frac{x}{\Delta x}$ where x is the output of the linear unit, and the input into the next non-linearity $\Gamma(\cdot)$. Shifting by s bits removes the 2^s scaling. We then use the activation table, indexed by $k + k_0$ where $k = \frac{x}{\Delta x}$ (the output from our sum/shift) and $k_0 = \text{index for } x = 0$. The values in the activation table are the index j_+ for the quantized activation, $a_{j_+} = \arg \min_j |\Gamma(k \Delta x) - a_j|$. If there is no following layer, we can look up that actual value of $\Gamma(k \Delta x)$ by looking up its value at in the LUT, using the value of i that corresponds to $w_i = 1$. No multiplications and no non-linearities are computed at inference time and all additions are integer. Note that the number of entries in the activation table can be more than N_a (the number of distinct quantized activation levels) if our nonlinearity does not change level at a uniform rate (e.g., quantized tanh). (Similar to Figure 9 in (Baluja et al., 2018), with permission.)

tions.¹ Figure 1 illustrates this approach. After quantization of weights and activations, the network is represented with three tables; Figure 1 shows two of them. The third table, the weight-index table, is also discussed below.

The first table, the LUT, provides the result of the multiplication between a quantized weight and its input, which is, itself, the output of the previous layer’s quantized activation function. This table contains $N_a N_w$ elements: the number of activation quantization levels, N_a , times the number of weight quantization levels, N_w . The value stored in each cell is the closest integer to $\frac{2^s}{\Delta x} w_i a_j$ where 2^s is the fixed-point scaling factor (allowing accurate accumulation) and Δx is the quantization step used in the activation table. We force the weight quantizations to include one; this also handles the bias elements. Additionally, the $w_i = 1$ column can be used to look-up the final layer’s actual output value.²

This LUT is different at each layer, if the quantization lev-

¹ Note that this approach does not require uniform quantization on either weights or activations.

² Similarly, to implement the scaling needed for average pooling, we can add a single-row for that specific scaling.

els for the different layers are not shared. If the network computation is scheduled by layer, then only the current layer’s LUT needs to fit into CPU L1 cache (or the FPGA block RAM) at a time, but there are time and energy costs to updating the tables between layers. We try to capture these two types of cost by breaking out the per-layer LUT size with NUC and the full network cost using NWNC.

The second table, the activation table, is of size N_x , where N_x is the number of Δx -sized steps needed in the activation-input space to fully span the quantized range of activation outputs. Assuming a standard, bounded, non-decreasing activation function, $\gamma(\cdot)$ (e.g., Tanh, Sigmoid, ReLu6), N_x is the count from the largest k giving $\arg \min_j |\gamma(k\Delta x) - a_j| = 0$ through (inclusive) the smallest k giving $\arg \min_j |\gamma(k\Delta x) - a_j| = N_a - 1$. For example, if $\gamma(\cdot)$ is Tanh, quantized to uniform output spacing $\frac{2}{N_a - 1}$ with $\Delta x = 0.02$ and $N_a = 32$, then $N_x = 207$ (across $x = \pm 2.06$). It is important to note here that the size of the LUT and the activation table are crucial for memory and bandwidth constrained systems.

With an FPGA implementation, ideally, both the LUT and activation table should simultaneously fit onto the distributed memory of the FPGA, since the order in which they will be accessed is not predictable. This is easier than the full LUT size would suggest, since only the one column of the LUT that corresponds to w_i (the weight that is used at that location in the network) needs to be accessed during each multiplication. For the purposes of FPGA access (where the processing and memory is distributed), this reduces the per-multiplication memory usage to N_a and the per-accumulator memory usage to N_x .

For the final classification decision, we retain the full precision of the accumulator instead of completing the “ $\ll s$ ”, indicated in Figure 1. We then find the index of the 1st (for recall@1) or top-5 (for recall@5) maximum output values. In this way, we do not lose ranking precision and we do not need to move to floating-point numbers.

The third table is the weight-index. For each of the network’s connections, this stores the quantized-weight index. This is the largest table; it has N_{net} entries, where N_{net} is the number of weights and biases within the network. Each of the N_{net} entries is $\lceil \log_2 N_w \rceil$ bits wide, (where N_w is the # of weight quantization levels).³ Fortunately, since the sequencing for the neural-network computation is both fixed and predictable, this table can be accessed in predefined sections efficiently. It does not need to fit directly on chip. Nonetheless, limiting the table size has secondary

³ The average size of the weight-index-table entries ($\lceil \log_2 N_w \rceil$) can be further reduced using variable-length encoding. However, since this study is focused on the on-chip table sizes and operations, we do not attempt to quantify the amount of additional compression available by that route.

benefits, since it impacts the number of total table accesses and network download size.

A note about network inputs: we handle the network inputs into the first layer either by quantizing the input values to the network’s activation quantization levels or by using a separate LUT for multiplying the network’s inputs by the same quantized weights as used elsewhere. Looking ahead, when we used the former approach, we saw a drop in accuracy of 0.0–0.3% from what is reported in Table 1. (Baluja et al., 2018) provides more details about the impact of input quantization on k-means-based weight quantization (Section 3.1) and Laplacian-model-based weight quantization (Section 3.2)

In summary, using the standard floating-point representations for comparison, our approach reduces the size of the overall network from $32N_{\text{net}}$ down to $N_{\text{net}} \log_2 N_w$ (for the weight table) + $(s + \log_2 N_x)N_a N_w$ (for the LUT) + $N_x \log_2 N_a$ (for the activation table). Since the values of N_w , N_a , and N_x are miniscule compared to N_{net} , there is an immediate reduction in network download/storage size by $\frac{32}{\lceil \log_2 N_w \rceil}$. Additionally, as we mentioned above, the LUT sizes provide intuitive measures with which to compare different quantization allocations and schemes.

2.2. Training Fully-Quantized Networks

To quantize the entire inference network, we broadly define two sets of quantization levels. The first set is used for the weights and bias units. The second set of levels is used for the activations. In its simplest form, the product of these two sets determines the NUC since it represents the total set of unique values that can be produced at any single layer or unit. Our goal is to minimize the set sizes of both, while also minimizing the impact to classification accuracy. To do this, we change the training process in two simple, localized steps, in the same way as was done in (Baluja et al., 2018).

The first modification allows backwards error-propagation through quantized activations. We use the “straight-through estimator” (STE) (Hinton, 2012), which has been widely used for quantization (Courbariaux et al., 2015; Zhou et al., 2016; Miyashita et al., 2016). Simply, this means that during training, the discretized activations use the gradients that would have been provided by the non-discretized version.

The second training modification allows us to find good weight and bias cluster centers. Using one of the methods from Section 3, we find new quantization centers once every S training steps⁴ (we set $S = 1000$). In each of these quantizing passes, we replace each weight (and bias) with its assigned quantization center. This temporarily reduces the number of unique weights and biases to N_w . After this

⁴Note that for the methods described in Section 3.3 and 3.4, the *cluster centers* will not change after the first quantization pass.

quantization event, training continues with no modifications until the next multiple-of- S training step. Between the quantization events, the weights diverge from the quantized levels. Nonetheless, these periodic reinforcements of the selected levels ensures that the final quantization event is not detrimental to performance. More details can be found in (Baluja et al., 2018).

2.3. Handling Batch-Norm for Quantization

One hurdle to quantization is batch-norm (BN) (Ioffe & Szegedy, 2015). The difficulty for quantization arises because BN moves the weights and biases of each unit independently. Most earlier quantization work has focused either on networks that are shallow enough that they can be trained without using BN or on quantization approaches that rescale quantization levels across layers (Jacob et al., 2018) and, often, even across channels (Krishnamoorthi, 2018). Unfortunately, the first (training without BN) limits the set of networks that we can consider. The latter (using different quantization scaling) increases the distinct quantization levels used by the weights and biases across the full network, giving much larger values for NWNC. By folding BN into the weights *before quantizing*, we can avoid both of these compromises.

We first train the network without quantization, using BN. Upon convergence, we fold the changes dictated by BN into the weight layers immediately preceding the normalization functions. We thereby eliminate the $1 \times 1 \times 1$ linear layer that BN would otherwise create. The BN changes to the weights and biases are combined with those of the basic convolutional unit, using the equations given in Appendix A, and the BN unit can be removed. We then measure the distribution of these “BN-folded” weights and biases (for Section 3.3) or the extremal values (for Section 3.4). The BN-folded weights and biases are then quantized using one of the approaches described next.

3. Weight quantization approaches

We present four approaches to weight/bias quantization. In this section, our activation quantization is uniform. For the purposes of being concrete, we compare these alternative quantization approaches using AlexNet (Krizhevsky et al., 2012). Our baseline accuracy with AlexNet (without quantization, using ReLU6) on ImageNet (Deng et al., 2009) is 56.4% / 79.8% (recall@1 / recall@5). More training and baseline-accuracy details will be given in Section 5.

3.1. Weight/bias quantization using 1-D k-means

Previous efforts in adaptive selection of weight quantizations have used k-means (Jain, 2010) on the weight vectors that make up the full kernels (Gong et al., 2014; Han et al.,

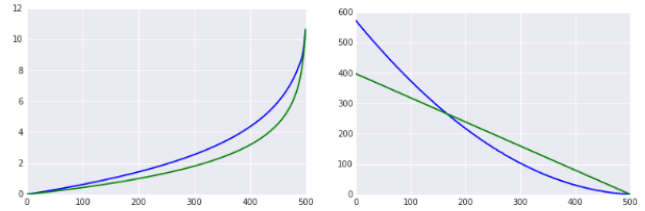


Figure 2. Quantization centers (left) and bin counts (right), for the upper half of a Laplacian distribution $\sigma = \sqrt{2}$, $N_w = 1000$, $N_{\text{net}} = 100,000$. Green minimizes L_1 quantization error; blue, L_2 error. Quantization centers are non-uniformly spaced with wider spacing at large amplitudes. (Reproduced with permission from (Baluja et al., 2018))

2015; Choi et al., 2017). (Baluja et al., 2018) took a simpler approach here and performed k-means clustering on weights and biases: in effect, one-dimensional clustering. Though the optimal solution can be found in $O(n^2k)$ (Wang & Song, 2011), because of the size of the networks considered ($> 5 * 10^7$ for AlexNet), (Baluja et al., 2018) instead used the standard k-means algorithm and subsampled the weight/biases to $n = 100,000$.

Using this approach with AlexNet, starting quantization training from scratch, using 1000 weight quantization levels (across *all* weights and biases in the network), and 32 linearly spaced activation levels with ReLU6, the classification accuracy is 52.5% (recall@1) and 76.3% (recall@5): a drop of 3.9% and 3.5%, respectively, from our baseline. The NUC, the set size of the possible outputs for each unit, is $32 * 1000 = 32,000$ and, since the same levels are used across the full network, the NWNC is also 32,000.

3.2. Quantization using a Laplacian distribution model

The k-means approach from Section 3.1 used subsampling to give a non-parametric estimate of the weight distribution. However, the weight distributions of a fully trained AlexNet appear to be nearly Laplacian (or, for some layers, Gaussian). This insight opens up novel model-based quantization approaches. Specifically, we can mathematically determine what the correct distribution of cluster centers and cluster occupancies should be to minimize *expected* L_1 or L_2 error for a Laplacian. We find this lowers the total error across the full weight set, compared to k-means on the 0.2% sample used in Section 3.1. Figure 2 shows these cluster centers and occupancies for a sample set drawn from a Laplacian distribution. More details are provided in Appendix B.

As in Section 3.1, we trained AlexNet from scratch and used 1000 weight/bias quantization levels and 32 linearly spaced ReLU6 activation levels (the same neural-unit complexity of 32,000 separate entries). We achieved 57.1% (recall@1) and 79.8% (recall@5). This is slightly *better* recall@1 than even the baseline, and the same recall@5 as the baseline. Both of these are better than k-means clustering (Section 3.1),

without increasing either NUC or NWNC.

3.3. Quantization using model-free distributions

If the optimal continuous-valued weights/biases are a sample from a single Laplacian distribution, we can minimize the expected L_1 (or L_2) error between the quantization centers and the optimal values using either a set of pre-computed cluster centers (Figure 2-a) or a set of pre-computed cluster occupancy counts (Figure 2-b). In Section 3.2, we used the pre-computed cluster centers. Here, we use the pre-computed cluster-occupancy counts. Figure 2-b shows that the occupancy counts for minimizing the expected L_1 Laplacian error is a (discretized) symmetric-about-zero triangle whose width is $N_w + 2$ and whose area is N_{net} : there are no scale parameters to be estimated. We simply collect, for each layer separately, the fully-trained, continuous-valued set of weights and biases; sort them; and assign them to the quantization bins according to the cumulative counts that are indicated by the integral of the discretized triangle shape. The cluster centers are computed as the median value for each bin (to minimize L_1 error in the bin) or as the mean value (for L_2 error).

We are relying on the observed distributions to determine the location of our cluster centers. So, we begin by first training the model *without discretization*. We then use the distribution of the trained, continuous-valued weights/biases, along with our Laplacian-inspired triangle-occupancy profile, to determine the cluster occupancy count and our cluster centers. (The complete procedure is described, with step-by-step pseudo-code, in Appendix C.1.) We freeze both the cluster centers and cluster occupancy counts for the remainder of the quantized training, to avoid the problem of the weight/bias distribution straying from those found during the continuous-valued training.

If we quantized once and discontinued training, there would be a large drop in classification accuracy. With AlexNet, in the *first* quantization pass to 256 levels, the recall@1 was 10% below the final accuracy obtained by fine tuning. So, we continue training, using this quantized starting point. As expected, with continued training, the quantized weights move away from the quantized values. Periodically (every 1000th step), we again sort the biases and weights and reassociate each with the cluster center that the triangle-occupancy profile dictates, regardless of whether that is the closest cluster center by L_1 distance. These weights/biases take on the value of the cluster center — the value that was determined (and frozen) based on our initial quantization. The individual weights/biases can change which cluster level they are quantized to, but the overall distribution is constant. Note the contrast with Sections 3.1 and 3.2.: both of those approaches re-clustered the weights/biases to whichever quantization level was closest, regardless of

occupancy counts.

This approach allows us to use units with lower complexity than before with no loss in recall@5 accuracy. Using 256 quantized weight/bias levels (instead of the 1000 previously) and 32 linearly spaced ReLU6 activation levels, the NUC is 8192 entries. However, since we do the clustering independently at each layer, the NWNC is less compact than our previous approaches: the NWNC is 65,524 entries. With this, the model-free-quantized AlexNet achieves 56.4% (recall@1) and 79.8% (recall@5). The recall@5 performance matches both the baseline (unquantized) AlexNet and the Laplacian-modeled quantization — with $\frac{1}{4}$ of the NUC.

3.4. Weight/bias quantization using octave sampling

While we were able to reduce the neural-unit complexity using the model-free approach, we still used a large lookup table (256×32 entries) and the NWNC actually got worse (by a factor of 2). In this section, we present an alternative approach: we constrain the weight cluster centers such that we can re-use entries in our table to represent distinct weights. The intuition is to use weights that have the following periodicity every N_q entries: in an ordered list of values to represent, every value at index i is simply a bit-shifted version of the base value at index $i \bmod N_q$. This is possible using values for the weights/biases that are separated by exact octaves: specifically, 0 and

$$\pm 2^{K_{\text{max}} - k} 2^{-n/N_q}$$

for $0 < n \leq N_q$ and $0 \leq k < N_o$ where $K_{\text{max}} = 2^{\lceil \log_2 v_{\text{max}} \rceil}$ and $N_o = \lceil \log_2 v_{\text{max}} \rceil - \lfloor \log_2 v_{\text{min}} \rfloor$, with $v_{\text{max}}/v_{\text{min}}$ as the maximum/minimum non-zero amplitude values represented. Pseudo-code for this octave-based weight quantization approach is given in Appendix C.2.

Using this approach, we can represent $2N_qN_o + 1$ (the +1 is for the 0 value) distinct quantized weights with a LUT that is only N_aN_q separate entries. This is a factor of $2N_o$ smaller than would be needed for that many unconstrained entries. While a reduction in the NUC and NWNC is accurate, since we are constraining our weight centers, using just that LUT size (N_aN_q entries) understates the unit’s (and the network’s) complexity. With just that measure, there is no accounting for the number of octaves used. To address this, we add another term to our neural complexity. With respect to trainable parameters, we have one additional parameter for each additional octave that we cover. So, for octave-based weight quantization (and linear activation quantization), our neural complexity is the LUT size (N_qN_a) plus the additional octave parameters ($N_o - 1$): $N_qN_a + N_o - 1$. For our octave-based approach, we use the same quantization levels throughout the network, so the NWNC is the same as the NUC ($N_qN_a + N_o - 1$).

We have observed that octave sampling is well matched to

the light-tailed distributions of our network weights/biases, especially on the outer 3–4 octaves. Octave sampling oversamples the central lobe compared to what Laplacian distributions dictate, but these values do not require additional LUT memory.⁵

With these quantization centers, we can represent the weight index using a sign bit (± 1), an octave (k), and a within-octave index (n).⁶ When retrieving the result of multiplying a quantized activation (a) with the weight, the LUT only needs to hold results for $a \times 2^{-n/N_q}$ (so $N_a N_q$ entries). The answer can then be determined by bit shifting the saved result by $K_{\max} - k$ bits and possibly inverting the sign.

We tested this approach with similar numbers of quantization levels as Section 3.3: 15 octaves with 8 weight/bias samples per octave and 32 linearly spaced ReLU6 activation levels. Although the number of weight/bias quantization levels are similar to what we used for model-free quantization (241 vs 256 levels), the LUT size needed has only 256 entries, in contrast to the 8,192 entries in the model free approach. The neural-unit complexity is increased from the basic LUT size by the 15 octaves that are used, giving a NUC of $32 \times 9 + 15 - 1 = 271$ entries. Even with this constrained representation of weights, octave-quantized AlexNet gives 56.4% (recall@1) and 79.8% (recall@5). This matches the performance of the model-free quantization.

This approach is similar to (Miyashita et al., 2016), but with more general spacing in the log-amplitude space. Using this approach with $N_q = 1$, $N_o = 32$, and $N_a = 16$, (Miyashita et al., 2016) reported an AlexNet recall@5 accuracy of 73.6%. Using our approach with the same parameters, we obtain an accuracy of 76.2%: a 2.6% improvement.

4. Activation Quantization Approaches

In this section, we compare the trade-offs between two alternative approaches to activation quantization: uniform linear quantization and octave-based quantization.

4.1. Uniform-linear activation quantization

To this point, we have used linearly-spaced quantization levels on our activations. Uniform linear quantization is well matched to the distribution of the activation values, largely due to the compressive mapping of the bounded activation function. As shown in Section 3.4, when we use 15 octaves with 8 levels/octaves for weight quantization with 32-level uniform-linear quantization of activations, we get 56.4% (recall@1) and 79.8% (recall@5) accuracy with

⁵It might still be worthwhile pruning the number of quantization levels for the lower-amplitude octaves, since this number does impact the size of the weight-index table.

⁶Weights that quantize to zero are dropped before being saved.

AlexNet. The NUC and NWNC (both at 271 entries) are the smallest that we have been able to use successfully, so far.

4.2. Octave-based activation quantization

By quantizing the weights/biases and activations using log-amplitude quantization, we can both avoid the multiplication LUT and use only fixed-point addition for multiplication, by operating in the \log_2 index space.

Multiplications between quantized weights and quantized activations become fixed-point additions. Multiplying a quantized activation (with $N_{q;a}$ samples per octave) by a quantized weight (with $N_{q;w}$ samples per octave) is the same as adding the quantized weight index, scaled by $\frac{N_{q;a}}{N_{q;w}}$, to the quantized activation index. As long as $N_{q;a}$ is a power of two times $N_{q;w}$, this combination can be done by bit shifting the weight index, followed by a fixed-point addition. Importantly, the large doubly-indexed multiplication LUTs are no longer needed and are replaced with two, much smaller, single-index tables, as described below.

To sum the weighted inputs into each unit, we move back into (and then out of) the linear amplitude space using two small look-up tables. One table, with $\max(N_{q;w}, N_{q;a})$ entries, converts from log to linear amplitudes. As long as $\frac{\max(N_{q;w}, N_{q;a})}{\min(N_{q;w}, N_{q;a})}$ is an integer, we can do this conversion exactly (to the precision of the table entry). A second table, with $4N_{q;a}$ entries, returns us into the log-amplitude space, after accumulation. Discussion of the mechanics of this approach to accumulation starting from log-amplitude and sign representations are provided in Appendix D.

Returning to our definition of NUC, the complexity of the octave/octave unit would be $\max(N_{q;w}, N_{q;a})$ (for the log-to-linear LUT) plus $4N_{q;a}$ (for the reverse LUT) plus the numbers of additional octaves that re-use those LUTs in the weight space ($N_{o;w} - 1$) and in the activation space ($N_{o;a} - 1$). So the NUC and NWNC are $\max(N_{q;w}, N_{q;a}) + 4N_{q;a} + N_{o;w} + N_{o;a} - 2$.

We now revisit AlexNet using 8 weight samples/octave for 15 octaves. In contrast with 56.4% (recall@1) using 32 *linearly-spaced* activation levels (reported earlier), we get only 55.2% (recall@1) using 96 *log-spaced* activation levels (specifically, 32 samples/octave for 3 octaves). This is a loss in performance compared to the linearly-quantized activations, although we actually increased the number of activation quantization levels. The distributions are poorly matched; this is also seen in (Miyashita et al., 2016). The NUC captures this, since the complexity for the octave/octave unit ($\max(32, 8) + 4 * 32 + 15 + 3 - 2 = 176$) is less than that of the octave/linear unit ($32 * 8 + 15 - 1 = 270$). (And the same for the NWNC.) If we think of LUT size as an indicator for neural complexity, we notice that because of the constraints, the effective size of the LUT is actually

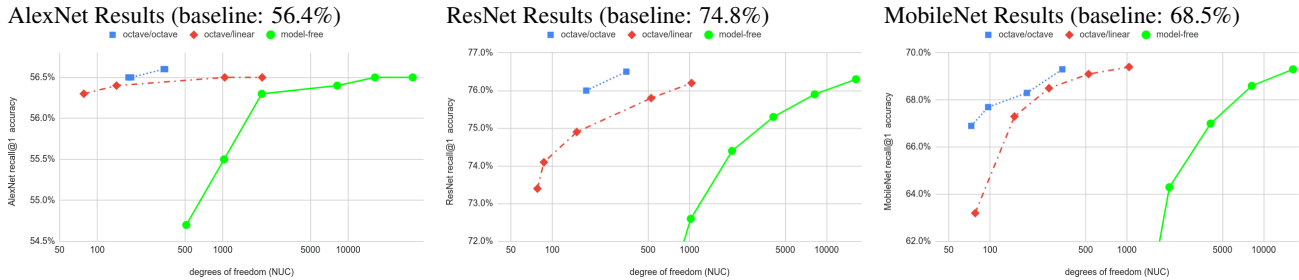


Figure 3. Accuracy versus Neural-Unit Complexity. The X-axis shows the number of trainable parameters per table-based neural unit as a measure of complexity. Note: the X-axis uses *log spacing*. If we had instead used NWN, “octave/octave” and “octave/linear” would have remained the same but “model free” would have slide to the right by a factor of 8, 101, and 28 for AlexNet, ResNet, and MobileNet, respectively.

much smaller. Therefore, the representational complexity of the unit is effectively smaller. In summary, we can replace all multiplications with additions and further reduce our minimal memory requirements but, when compared on the basis of quantization levels alone, there is a performance degradation of 5.6% or more.

Finally, comparing our AlexNet results to those in (Miyashita et al., 2016): with $N_{q:w} = 2$ and $N_{q:a} = 1$, we get 79.0% recall@5 while (Miyashita et al., 2016) gets 75.1% recall@5 when using octave/octave quantization in that operating regime. Additionally, Figure 3 shows that the peak performance of this octave/octave neural unit was better than the octave/linear neural unit *at the same NUC* but worse than the octave/linear neural unit when compared at the same total number of activation levels.

5. Large-Scale Experiments

In this section, we further test our model-free and octave-based approaches. We use AlexNet, ResNet-101, and MobileNet. We create a “pre-trained” model of each network from scratch with ReLU and with ReLU6 units. All models are trained on the ImageNet 2012 training set and recall@1 and @5 are computed on the validation set using the 10-crop procedure (Krizhevsky et al., 2012). For these experiments, the quantization networks are fine-tuned from the pre-trained model. The baselines are the ReLU6 models.

AlexNet: AlexNet is most useful for comparison to prior work. We follow the training procedures specified in (Krizhevsky et al., 2012), except: we use RMSProp; initial weight sd=0.005; bias initializer sd=0.1; one Tesla-V100 GPU; and a stepwise decaying learning rate (LR). Our ReLU network achieved accuracies: recall@1 of 57.4% and recall@5 of 80.4%. (Krizhevsky et al., 2012) reported 59.3% and 81.8%, recall@1 and @5, respectively. The small difference was because we did not use the PCA pre-processing or LRN (Krizhevsky et al., 2012). Our ReLU6 baseline results: 56.4% recall@1 and 79.8% recall@5. Fine-tuning is done from this model with LR starting at 0.0001.

ResNet-101: We selected ResNet (He et al., 2015) as a modern deep network that takes full advantage of non-separable convolutional kernels. For our implementation: 8 GPUs splitting a mini-batch size of 256; and cosine rate decay (Loschilov & Hutter, 2016) ending after 300,000 steps. Our ReLU model achieved a recall@1 accuracy of 77.8% and recall@5 accuracy of 94.1%. (He et al., 2015) reported accuracies of 78.25% and 93.95%. Training with ReLU6, our baseline, we see 74.8% and 92.3%. We fine-tune from the ReLU network with LR starting at 0.0001.

MobileNet: MobileNet is a compact network for mobile deployment. We followed (Howard et al., 2017) except: 4 GPUs splitting a mini-batch size of 96; and a LR-decay of 0.98 every 13346 steps. Our network had a recall@1 accuracy of 68.4% and @5 of 88.0%. (Howard et al., 2017) reported 70.6% recall@1. Our baseline ReLU6 net saw 68.5% @1 and 88.0% @5. Fine-tuning is from this network with LR-cosine decay starting at 0.0001 for 500,000 steps.

Figure 3 compares the accuracy of our different approaches (model-free, octave/linear, and octave/octave) based on the NUC degrees of freedom in each layer. The plot shows the “efficient frontier” for the trade-off in the way that the degrees of freedom are allocated. For example, in the AlexNet results, for the model-free approach, when the NUC is below 1024 entries, it is best to use 8 activation levels, above that, it uses 16 levels (through 4096 entries), then 32 levels. Other allocations of NUC did not do as well. Even though the octave/octave has the fewest degrees of freedom, it achieves the highest recall@1 (and recall@5) accuracy on both AlexNet and ResNet. Octave/linear gives slightly better recall@1 accuracy on MobileNet but does so using 3× the degrees of freedom. Similar changes in the best activation quantization levels were seen in octave/linear and octave/octave results.

For octave/linear results, in the range of 4–32 weights/octave, we found that the most effective $N_{o:w}$ was closely tied to the step size used for the activation quantization. If a non-zero weight was so small that having it multiply the maximum activation value would only move

the accumulated result by at most $\frac{1}{2}$ the activation step size, changing that weight to zero did not make a measurable degradation to the overall accuracy. Instead, it was better to reduce $N_{o:w}$ for that choice of activation quantization. We observed similar trends for the octave/octave results.

Table 1 provides a thorough comparison of our results with prior work in quantizing both activations and weights on AlexNet, ResNet, or MobileNet. After the name column, we use eight columns to describe the quantization paradigm. In the first column, we show whether the approach used bit-shifts or floating/fixed-point multiplies. In column “Quant first, last, bias”, we specify exactly what was quantized - were the first and last layer and bias unit quantized? Then we give the NUC (and the per-layer LUT size, if it differs from the NUC) and the NWNC (and the network-wide combined LUT size, if it differs) as indications of the degrees of freedom and memory constraints. The next 2 columns give the quantization levels for the weights and activations. “Per-unit N_w / N_a ” are the numbers of distinct weight & activation levels *seen by any unit in the network*. “Full-net N_w / N_a ” are the numbers of distinct weight & activation levels *across the full network*.

The results are shown in the the last two sections of the table (last 6 columns). They give the baseline performance of all the methods and how their quantization affects performance - measured at recall @1 and @5. Though there is an overwhelming amount of information in the table, perhaps most interestingly, our quantized results often either remain consistent or even *improve* over the ReLU6 baseline.

Note that the detailed characterization of the the quantization of different approaches is necessary due to the breadth of approaches to quantization. For all our networks except model-free, the distinct quantization levels are shared *throughout the whole network*. (Model-free quantizes each layer independently.) Many of the previous approaches to quantizing AlexNet use only two or three levels per layer but then scale each of the eight layers separately (Zhou et al., 2016; Wu et al., 2018; Rastegari et al., 2016; Hubara et al., 2016).

To summarize, all three of our approaches were better than previous results on AlexNet. For ResNet and MobileNet, our results are nearly identical to those of (Jacob et al., 2018): we are 0.1% better on MobileNet but 0.1% worse on ResNet. We use fewer levels (both weights and activations) than were used in (Jacob et al., 2018) but, using the freedom given by our table-based approach (Figure 1), we are able to place our levels more strategically than is possible using simple fixed-point representations. Remember, also, that our table-based approach removes all multiplications, unlike (Jacob et al., 2018), opening up highly efficient FPGA implementations (Garland & Gregg, 2017).

Finally, two other interesting results from MobileNet are the extremely compact versions that are listed on lines 22-23 of Table 1. Using absolutely no multiplication or floating point, using only 40 entries (across the two LUTs), we achieved 66.9% recall@1: just 1.6% below our baseline. If we allow ourselves 64 entries, we cut the loss in half for 67.7% recall@1, 0.8% below our baseline. With these versions, we are well within what can fit into on-chip registers.

6. Conclusions

Our studies have focused on quantifying neural-unit complexity (NUC) and network-wide non-compactness (NWNC). We examined how to best lower both of these measures without impacting classification accuracy. Our definitions of NUC & NWNC are very closely tied to the number of trainable parameters and unique values *at each layer* and *across the full network*, respectively. We obtained improved results over the numerous previous approaches we examined, even though we quantized more of the network - we *completely* quantized the weights, the biases and the quantizations. Perhaps what is the most surprising aspect of this study is the small number of unique values needed to represent the weights and activations across the entire network. For AlexNet, we achieve 56.5% recall@1 and 80.0% recall@5 with only 347 unique values. On ResNet, our best performance is 76.5% recall@1 and 93.3% recall@5, again with only 347 values. On MobileNet, our two best results are 69.3% recall@1 / 88.5% recall@5 with 338 values and 69.4% / 88.5% with 1038 values. Using our table-based approach, these resulting tiny tables allow for in-memory caching and require no floating point representation. Additionally, as described, we can eliminate all multiplications as well. These are all achieved without sacrificing classification performance.

Table 1. Accuracy under Quantization: Comparison to Prior Work.

Key for the “multiplies?” column: *FP* = some floating-point multiplies in inference; *fp* = fixed-point multiplies; \ll = scaling by a power of two (e.g. bit shifts). Key for “NUC $\lceil \lceil \text{LUT} \rceil_{lay} \rceil$ ” column: neural-unit capacity, in terms of trainable parameters, accessible at a single layer and the per-layer LUT size, if it differs. Key for “NWNC $\lceil \lceil \text{LUT} \rceil_{net} \rceil$ ” column: network-wide non-compactness and network-wide count of distinct LUT entries, if it differs; $+FP$ = some floating-point portions not accounted for in the trainable-parameters count. (See main text for definitions.)

		Quantization Description					Recall@1			Recall@5		
		Quant first,last, (bias < 2 ³²)	NUC $\lceil \lceil \text{LUT} \rceil_{lay} \rceil$ if differ]	NWNC $\lceil \lceil \text{LUT} \rceil_{net} \rceil$ if differ]	per-unit N_w / N_a	full-net N_w / N_a	base- line	quant.	diff.	base- line	quant.	diff.
AlexNet												
1	Our work											
2	Model-free		16,384	131,072	512 / 32	4096 / 32	56.4%	56.5%	+0.1%	79.8%	79.9%	+0.1%
3	Octave/linear		1038 / 1024	1038 / 1024	481 / 64	481 / 64		56.5%	+0.1%		79.8%	0.0%
4	Octave/octave		347 / 320	347 / 320	385 / 321	385 / 321		56.6%	+0.2%		80.0%	+0.2%
5	(Wu et al., 2018)		512 or FP	526 + FP	3 / 255	24 / 2040	-	-	-		80.7%	-4.8%
6	(Miyashita et al., 2016) [†]		288 / 4	296 / 32	256 / 16	1,632 / 128	-	-	-		78.3%	-2.7%
7	(Zhou et al., 2016) [‡]		65,536 + FP	65,550 + FP	256 / 256	2048 / 2048	55.9%	53.0%	-2.9%	-	-	-
8	(Hubara et al., 2016) [‡]		8 or FP	22 + FP	2 / 4	16 / 32	56.6%	51.0%	-5.6%	80.2%	73.7%	-6.5%
9	(Rastegari et al., 2016)		4 or FP	18 + FP	2 / 2	16 / 16	56.6%	44.2%	-12.4%	80.2%	69.2%	-11.0%
ResNet												
10	Our work											
11	Model-free/linear		16,384	1,654,784	512 / 32	51,712 / 32	74.8%	76.3%	+1.5%	92.3%	93.2%	+0.7%
12	Octave/linear		8,192	827,392	256 / 32	25,856 / 32		75.9%	+1.1%		93.0%	+0.7%
13	Octave/octave		2062 / 2048	2062 / 2048	961 / 64	961 / 64		76.2%	+1.4%		93.2%	+0.9%
14	Octave/octave		526 / 512	526 / 512	241 / 64	241 / 64		75.2%	+0.4%		92.7%	+0.4%
15	(Jacob et al., 2018) [§]		347 / 320	347 / 320	1537 / 321	1537 / 321		76.5%	+1.7%		93.3%	+1.0%
16	(Jacob et al., 2018)		65,536	65,736	256 / 256	25,856 / 25,856	78.0%	76.6%	-1.4%	-	-	-
MobileNet												
17	Our work											
18	Model-free/linear		16,384	1,835,008	256 / 64	7,168 / 64	68.5%	69.3%	+0.8%	88.0%	88.6%	+0.6%
19	Octave/linear		1038 / 1024	1038 / 1024	482 / 64	481 / 64		69.4%	+0.9%		88.5%	+0.5%
20	Octave/octave		526 / 512	526 / 512	241 / 64	241 / 64		69.1%	+0.6%		88.4%	+0.4%
21	Octave/octave		338 / 320	338 / 320	961 / 321	961 / 321		69.3%	+0.8%		88.5%	+0.5%
22	(Zhou et al., 2016)		73 / 40	73 / 40	497 / 33	497 / 33		66.9%	-1.6%		86.9%	-1.1%
23	(Zhou et al., 2016)		97 / 64	97 / 64	1985 / 33	1985 / 33		67.7%	-0.8%		87.3%	-0.7%
24	(Jacob et al., 2018) [§]		65,536	65,592	256 / 256	7,168 / 7,168	70.5%	69.3%	-1.2%	-	-	-

[†] For (Miyashita et al., 2016), NUC is for Conv3 layer, the widest and full-net N_a and N_w include both numbers of octaves and per-layer scaling.

[‡] For (Zhou et al., 2016): Bias-count answer based on (Wu & Zou, 2018).

[§] For (Hubara et al., 2016): FP operations needed in the “approximate batch-norm” (AP2) that they add before the first layer.

References

- Achterhold, J., Koehler, J. M., Schmeink, A., and Genewein, T. Variational network quantization. In *International Conference on Learning Representations (ICLR)*, 2018.
- Anwar, S., Hwang, K., and Sung, W. Fixed point optimization of deep convolutional neural networks for object recognition. In *Proceedings of the IEEE International Conference on Acoustics, Speech and Signal Processing (ICASSP)*, 2015.
- Baluja, S., Marwood, D., Covell, M., and Johnston, N. No multiplication? no floating point? no problem! training networks for efficient inference. *arXiv preprint*, 2018.
- Balzer, W., Takahashi, M., Ohta, J., and Kyuma, K. Weight quantization in Boltzmann machines. *Neural Networks*, 4(3):405–409, 1991.
- Cai, Z., He, X., Sun, J., and Vasconcelos, N. Deep learning with low precision by half-wave gaussian quantization. In *Computer Vision and Pattern Recognition (CVPR)*, 2017.
- Chatterjee, S. Learning and memorization. In *International Conference on Machine Learning*, 2018.
- Choi, Y., El-Khamy, M., and Lee, J. Towards the limit of network quantization. In *International Conference on Learning Representations (ICLR)*, 2017.
- Courbariaux, M., Bengio, Y., and David, J.-P. BinaryConnect: Training deep neural networks with binary weights during propagations. In *Advances in Neural Information Processing Systems*, 2015.
- Courbariaux, M., Hubara, I., Soudry, D., El-Yaniv, R., and Bengio, Y. Binarized neural networks: Training deep neural networks with weights and activations constrained to +1 or -1. *arXiv preprint arXiv:1602.02830*, 2016.
- Deng, J., Dong, W., Socher, R., Li, L.-J., Li, K., and Fei-Fei, L. Imagenet: A large-scale hierarchical image database. In *Computer Vision and Pattern Recognition, 2009. CVPR 2009. IEEE Conference on*, pp. 248–255. IEEE, 2009.
- Deng, L., Jiao, P., Pei, J., Wu, Z., and Li, G. Gated XNOR networks: Deep neural networks with ternary weights and activations under a unified discretization framework. *CoRR*, abs/1705.09283, 2017. URL <http://arxiv.org/abs/1705.09283>.
- Garland, J. and Gregg, D. Low complexity multiply-accumulate units for convolutional neural networks with weight-sharing. *IEEE Computer Architecture Letters*, 2017.
- Gong, Y., Liu, L., Yang, M., and Bourdev, L. Compressing deep convolutional networks using vector quantization. *arXiv 1412.6115*, 2014.
- Guo, Y. A survey on methods and theories of quantized neural networks. *arXiv 1808.04752*, 2018.
- Han, S., Mao, H., and Dally, W. Deep compression: Compressing deep neural networks with pruning, trained quantization and huffman coding. *arXiv 1510.00149*, 2015.
- Han, S., Mao, H., and Dally, W. J. Deep compression: Compressing deep neural networks with pruning, trained quantization and huffman coding. *International Conference on Learning Representations (ICLR)*, 2016.
- He, K., Zhang, X., Ren, S., and Sun, J. Deep residual learning for image recognition. *CoRR*, abs/1512.03385, 2015. URL <http://arxiv.org/abs/1512.03385>.
- Hinton, G. Neural networks for machine learning. Coursera, video lectures, 2012.
- Howard, A., Zhu, M., Chen, B., Kalenichenko, D., Wang, W., Weyand, T., Andreetto, M., and Adam, H. Mobilenets: Efficient convolutional neural networks for mobile vision applications. *arXiv 1704.04861*, 2017.
- Hubara, I., Courbariaux, M., Soudry, D., El-Yaniv, R., and Bengio, Y. Quantized neural networks: Training neural networks with low precision weights and activations. *arXiv arXiv:1609.07061*, 2016.
- Hwang, K. and Sung, W. Fixed-point feedforward deep neural network design using weights +1, 0, and -1. In *Workshop on Signal Processing Systems (SiPS)*, 2014.
- Ioffe, S. and Szegedy, C. Batch normalization: Accelerating deep network training by reducing internal covariate shift. In *Proc. International Conference on Machine Learning*, pp. 448–456, 2015.
- Jacob, B., Kligys, S., Chen, B., Zhu, M., Tang, M., Howard, A., Adam, H., and Kalenichenko, D. Quantization and training of neural networks for efficient integer-arithmetic-only inference. In *Computer Vision and Pattern Recognition (CVPR)*, 2018.
- Jain, A. K. Data clustering: 50 years beyond k-means. *Pattern recognition letters*, 31(8):651–666, 2010.
- Kim, J., Hwang, K., and Sung, W. X1000 real-time phoneme recognition VLSI using feed-forward deep neural networks. In *International Conference on Acoustics, Speech and Signal Processing (ICASSP)*, 2014.
- Krishnamoorthi, R. Quantizing deep convolutional networks for efficient inference: A whitepaper. *arXiv 1806.08342*, 2018.
- Krizhevsky, A., Sutskever, I., and Hinton, G. E. Imagenet classification with deep convolutional neural networks. In *Advances in neural information processing systems*, pp. 1097–1105, 2012.

- Langhammer, M. and Baeckler, G. High density and performance multiplication for fpga. In *IEEE Symposium on Computer Arithmetic*, 2018.
- Li, H., De, S., Xu, Z., Studer, C., Samet, H., and Goldstein, T. Training quantized nets: A deeper understanding. In *Advances in Neural Information Processing Systems*, 2017.
- Lin, D. D., Talathi, S. S., and Annapureddy, V. S. Fixed point quantization of deep convolutional networks. *CoRR*, abs/1511.06393, 2015. URL <http://arxiv.org/abs/1511.06393>.
- Loschilov, I. and Hutter, F. Sgdr: Stochastic gradient descent with warm restarts. *arXiv 1608.03983*, 2016.
- Marchesi, M., Orlandi, G., Piazza, F., and Uncini, A. Fast neural networks without multipliers. *IEEE transactions on Neural Networks*, 4(1):53–62, 1993.
- Marcus, G. Open cores project fpvhd1: Floating point adder and multiplier, 2004. URL <https://opencores.org/projects/fpvhd1>.
- Miyashita, D., Lee, E., and Murmann, B. Convolutional neural networks using logarithmic data representation. *arXiv 1603.01025*, 2016.
- Rastegari, M., Ordonez, V., Redmon, J., and Farhadi, A. XNOR-net: Imagenet classification using binary convolutional neural networks. In *European Conference on Computer Vision*, pp. 525–542. Springer, October 2016.
- Sabeetha, S., Ajayan, J., Shriram, S., Vivek, K., and Rajesh, V. A study of performance comparison of digital multipliers using 22nm strained silicon technology. In *Proc. International Conference on Electronics and Communication Systems (ICECS)*, pp. 180184, 2015.
- Salimans, T. and Kingma, D. P. Weight normalization: A simple reparameterization to accelerate training of deep neural networks. In *Proceedings of the 30th International Conference on Neural Information Processing Systems, NIPS’16*, 2016. URL <http://dl.acm.org/citation.cfm?id=3157096.3157197>.
- Tang, C. Z. and Kwan, H. K. Multilayer feedforward neural networks with single powers-of-two weights. *IEEE Transactions on Signal Processing*, 41(8):2724–2727, 1993.
- Tang, W., Hua, G., and Wang, L. How to train a compact binary neural network with high accuracy? In *AAAI Conference on Artificial Intelligence*, 2017.
- Vanhoucke, V., Senior, A., and Mao, M. Improving the speed of neural networks on cpus. In *NIPS Workshop on Deep Learning and Unsupervised Feature Learning*, 2011.
- Wang, H. and Song, M. Ckmeans. 1d. dp: optimal k-means clustering in one dimension by dynamic programming. *The R journal*, 3(2):29, 2011.
- Warren, Jr., H. Hacker’s delight: Number of leading zeros, 2013. URL <http://www.hackersdelight.org/hdcodetxt/nlz.c.txt>.
- Wu, S., Li, G., Chen, F., and Shi, L. Training and inference with integers in deep neural networks. *arXiv preprint arXiv:1802.04680*, 2018.
- Wu, Y. and Zou, Y. `tensorpack/examples/dorefa-net/alexnet-dorefa.py` - `github`. <https://github.com/tensorpack/tensorpack/blob/master/examples/DoReFa-Net/alexnet-dorefa.py>, 2018.
- Xilinx. 7 series fpgas data sheet: Overview (ds180), 2018. URL https://www.xilinx.com/support/documentation/data_sheets/ds180_7Series_Overview.pdf.
- Yi, Y., Hangping, Z., and Bin, Z. A new learning algorithm for neural networks with integer weights and quantized non-linear activation functions. In *IFIP International Conference on Artificial Intelligence in Theory and Practice*, pp. 427–431. Springer, 2008.
- Zhou, A., Yao, A., Guo, Y., Xu, L., and Chen, Y. Incremental network quantization: Towards lossless cnns with low-precision weights. In *International Conference on Learning Representations (ICLR)*, 2017.
- Zhou, S., Wu, Y., Ni, Z., Zhou, X., Wen, H., and Zou, Y. DoReFa-net: Training low bitwidth convolutional neural networks with low bitwidth gradients. *arXiv arXiv:1606.06160*, June 2016.
- Zhu, C., Han, S., Mao, H., and Dally, W. J. Trained ternary quantization. *arXiv 1612.01064*, 2016.

A. Quantization with Batch-Norm and Weight Norm: Implementation Details

As pointed out in Section 2.3, Batch norm (BN) (Ioffe & Szegedy, 2015) makes it difficult to train quantized networks since normalization moves the weights and biases of each unit independently. To avoid the compromises that an ongoing BN process would impose on our quantized network, we instead train with BN in the continuous-weight domain and only work towards a quantized network after the continuous-weight version has converged. Once the network has converged, we fold the changes dictated by the normalization operations into the weight-layers immediately preceding or following the normalization functions.

Using a variation on the notation from (Ioffe & Szegedy, 2015), BN changes each input x to y via

$$\begin{aligned} y &= \frac{\gamma}{\sigma}x + \left(\beta - \frac{\gamma}{\sigma}m\right) \\ \sigma &= \sqrt{\text{Var}[x] + \epsilon} \\ m &= E[x] \\ \gamma, \beta &\text{ are the BN learned parameters} \end{aligned}$$

When the BN operation is immediately *after* a weight layer, then that weight layers biases (b) and weights (w) change to

$$\begin{aligned} b &\leftarrow \frac{\gamma}{\sigma}b + \beta - \frac{\gamma}{\sigma}m \\ w &\leftarrow \frac{\gamma}{\sigma}w \end{aligned}$$

If the BN is immediately *before* a weight layer, then there are likely to be many different BN layers, each feeding into a different weight connection (w_i^+). Using i on the BN parameters to distinguish these different normalizations, folding all of the preceding BN's gives us:

$$\begin{aligned} b^+ &\leftarrow b^+ + \sum_i (\beta_i - \frac{\gamma_i}{\sigma_i} m_i) w_i^+ \\ w_i^+ &\leftarrow \frac{\gamma_i}{\sigma_i} w_i^+ \end{aligned}$$

(in that order).

Note that, if the batch norm feeds a skip connection or a tower split, the weights/biases for all of the convolutional layers that are directly connected to it need to be modified in the way just described.

For weight normalization (Salimans & Kingma, 2016), we can use basically the same formulas as above, but replacing $\frac{\gamma}{\sigma}$ with the weight normalization scaling (s) and replacing $\beta - \frac{\gamma}{\sigma}m$ with zero.

At the start of fine-tuning, the model is reconstructed without batch-norm. If associated weight layer, in the original network did not have a bias tensor (which they often do

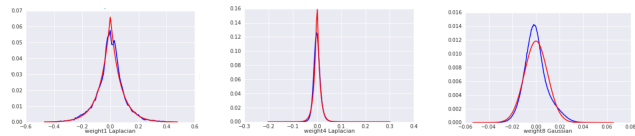


Figure 4. Histograms of weights from a well-trained (continuous) AlexNet, from layers 1, 4, and 8. The blue line is the actual weight distribution; the red one is the best fitting distribution (either Laplacian or Gaussian). The distributions of layers 2, 3, and 5 look very similar to the Laplacian distribution of layer 4. The distributions of layers 6 and 7 are similar to the Gaussian distribution of layer 8 with smaller variances. (Reproduced with permission from (Baluja et al., 2018))

not when associated with a BN layer), an initially-zero bias tensor is added to the weight layer. The pre-trained batch-norm parameters are folded into the pre-trained weights and biases. Training continues, with periodic quantization (according to one of the quantization approaches described in the main paper) and without any batch-norm computation.

B. Weight/bias quantization using a Laplacian distribution model

As asserted in Section 3.2 and shown in Figure 4, many fully-trained weight distributions resemble Laplacian or Gaussian distributions. This insight can help us to better select cluster centers and cluster occupancies.

If we have a sample from a Laplacian distribution and if it is small enough to cluster using the dynamic-programming implementation of 1-D k-means clustering then that method will provide the optimal clusters for that sample. However, with millions of weights (which are the samples we are trying to cluster), we can not do that. Instead, we can find the best clusters for the *expected* L_1 or L_2 error across all fair samples. Figure 2 (repeated here for ease of reference) shows cluster centers and occupancies for Laplacian distributions that minimize its L_1 or L_2 error in the weight/bias space.

One interesting characteristic of the L_1 Laplacian-based clustering model is that we can describe the best cluster center locations in closed form, as a function of the near-extreme values that were seen in the weight/bias set. We can also express the best cluster occupancies, as a function of the sample size and the number of clusters. Specifically, for the cluster centers with minimum expected L_1 error (using an odd number, N , of cluster centers), the cluster centers should be at $\pm bL_i$ where b is a scaling factor and where

$$\begin{aligned} L_i &= L_{i-1} + \Delta_i \\ \Delta_i &= -\ln(1 - 2 \exp(L_{i-1})/N) \\ L_0 &= 0 \end{aligned}$$

We set the scaling factor, b , using the cluster occupancy curve for guidance. From Figure 2-b, for minimum L_1 error on a fair sample set from a Laplacian distribution, occupancy of the clusters should fall linearly from the central peak of $\frac{2}{N}N_w$ to the outer most bins at $\frac{2}{N^2}N_w$. Using this insight, we set $b = W_{max}/L_{N/2}$ where W_{max} is based on the weight magnitudes in the outer half of the outermost quantization bins.

We gave the description for the cluster occupancy with the minimum expected L_1 error in Subsection 3.3. Repeating that here: The cluster occupancy counts which minimize the expected L_1 Laplacian error is a (discretized) symmetric-about-zero triangle whose width is $N_w + 2$ and whose area is N_{net} . For the cluster counts (unlike the cluster centers), there are no scale parameters to be estimated.

Since some of the layers' weight distributions are closer to Gaussian than Laplacian (for example, layer 8 of AlexNet, shown in Figure 4), we need to consider this model mismatch. However, using the Laplacian occupancy profile works well for both Laplacian and Gaussian distributions: the increase in L_1 error caused by using the Laplacian profile on a Gaussian distribution is under 4%. The Laplacian occupancy profile does not work as well for heavy-tailed distributions, like the Cauchy distribution, resulting in 51% more error than could have been achieved by using the correct probability profile. However, none of the weight distributions that we have encountered in our network training were heavy tailed.

We give our results using this Laplacian-model approach in Subsection 3.2.

C. Pseudo-code for Weight quantization approaches

Due to the simplicity of the 1-D k-means weight clustering, we do not include pseudo-code for that approach. Since we dropped the Laplacian quantization approach for our later studies, we do not include pseudo-code for that approach, just the mathematical description in Appendix B.

C.1. Weight/bias quantization using a non-parametric probability distribution model

The code for Section 3.3 is in Algorithm 1.

C.2. Weight/bias quantization using Octave

The code for Section 3.4 is in Algorithm 2.

D. Addition under octave-based quantization for both activation outputs and weights/biases

In much of the paper, we have used linearly spaced quantization levels, which we (and others (Miyashita et al., 2016)) have found is better matched to the distributions of activation-output values than is octave-based quantization. However, if we quantize our weights/biases **and** the activation outputs using uniform log-amplitude quantization, there are two benefits. We can:

- replace the multiplication (double indexed) LUT of size $N_a N_w$ by two much smaller (single-index) tables. The first smaller table is used to move out of log-linear space to linear amplitude space, and is of size $\max(N_{q;a}, N_{q;w})$. The second table to reverse this mapping is of size $4N_{q;a}$.
- use only fixed-point addition to complete the multiplication, by operating in the \log_2 index space.

Multiplications between quantized weights and quantized activation outputs become fixed-point additions: using the notation,

$$\begin{aligned} s_x &= \text{sign}(x) \\ v_x &= \text{round}(N_{q;x} \log_2(|x|)) \end{aligned}$$

where $N_{q;x}$ is the number of equally spaced samples per octave that we are using for x , then for a v_{wa} quantized to $N_{q;a}$ samples per octave:

$$\begin{aligned} s_{wa} &= \text{sign}(wa) = s_w s_a \\ v_{wa} &= \text{round}(N_{q;a} \log_2(|wa|)) \\ &= \text{round}(N_{q;a} \log_2(2^{v_w/N_{q;w}} 2^{v_a/N_{q;a}})) \\ &= v_a + v_w \frac{N_{q;a}}{N_{q;w}} \end{aligned}$$

As long as $N_{q;a}$ is a power of two $\times N_{q;w}$, this combination can be done using a bit shift of v_w followed by a fixed-point addition.

To add together the weighted inputs from the network, we temporarily move back into (and then out of) the linear amplitude space, using two singly-indexed LUTs of combined size $\max(N_{q;a}, N_{q;w}) + 4N_{q;a}$. We chose to do this instead of using a Taylor-series approximation (Miyashita et al., 2016) for accuracy. Figure 5 shows the error between $\log_2(1+x)$ and its first-order Taylor-series expansion around $x = 0$ for the range from -1 to 1, which is the range needed to use this expansion as the basis for linear-value addition in the log domain. However, as can be seen by Figure 5, that approximation does not work well when the

Algorithm 1 Model-Free Weight Quantization Pseudo-Code: Training

Throughout, fully-connected layers are implemented as conv2d layers with a 1x1 kernel.

{***INITIALIZATION***}

Input: N_q : The number of weights; *model*: a pre-trained model; *cut_values*: a dictionary from the conv layer tensors in *model* to a list of indices.

- 1: **for all** *batch_norm_layer* \in *model* **do**
- 2: Fold *batch_norm_layer* into the preceding conv layer (see Section 2.3).
- 3: **end for**
- 4: {*ConvLayerTensors*(*model*) returns all the conv layer tensors in model, both weights and biases.}
- 5: {Build *quantized_values*, a dictionary from each tensor in *ConvLayerTensors*(*model*) to its sorted, quantized values.}
- 6: {The input *cut_values*[*tensor*] is a list of indices. *cut_values*[*tensor*][*i* + 1] – *cut_values*[*tensor*][*i*] is the number of values in tensor that belong in bucket *i*, for *i* = 0 to N_q .}
- 7: **for all** *tensor* \in *ConvLayerTensors*(*model*) **do**
- 8: *sorted_tensor* \leftarrow *sort*(*tensor.flatten*())
- 9: **for** *i* = 0 to N_q **do**
- 10: *cut_start* = *cut_values*[*i*]
- 11: *cut_end* = *cut_values*[*i* + 1]
- 12: *centroid* \leftarrow *average*(*sorted_tensor*[*cut_start* : *cut_end*])
- 13: *quantized_values*[*tensor*] \leftarrow *quantized_values*[*tensor*] + [*centroid*] * (*cut_end* – *cut_start*)
- 14: **end for**
- 15: **end for**

Output: *quantized_values*; *model*

{***EVERY 1000 TRAINING STEPS***}

Input: *quantized_values*; *model*

- 16: **for all** *input_tensor* \in *ConvLayerTensors*(*model*) **do**
 - 17: {Assign the *quantized_values* from the initial model into the tensors.}
 - 18: *arg_sorted* = *argsort*(*input_tensor.flatten*())
 - 19: *quantized_tensor* \leftarrow *scatter*(*quantized_values*[*input_tensor*], *arg_sorted*)
 - 20: *input_tensor* \leftarrow *quantized_tensor.reshape*(*input_tensor.shape*)
 - 21: **end for**
 - 22: Save *model*, the quantized checkpoint.
-

Algorithm 2 Octave Weight Quantization Pseudo-Code

Throughout, fully-connected layers are implemented as conv2d layers with a 1x1 kernel.

```
{**** Compute a codebook of all the quantized values. ****}
```

Input: N_o : number of octaves; N_q : number of quantization levels within each octave; K_{max} : maximum quantized value

 1: $codebook \leftarrow K_{max} \times pow(2, range(-N_q \times N_o - 1, 1)/N_q)$

 2: $codebook \leftarrow -flip(codebook) + [0] + codebook$
{Explanation: Tensor values in the range $(cut_values[i], cut_values[i + 1])$ will be quantized to $codebook[i + 1]$.
 Values less than $cut_values[0]$ are quantized to $codebook[0]$.
 Values greater than $cut_values[-1]$ are quantized to $codebook[-1]$.}

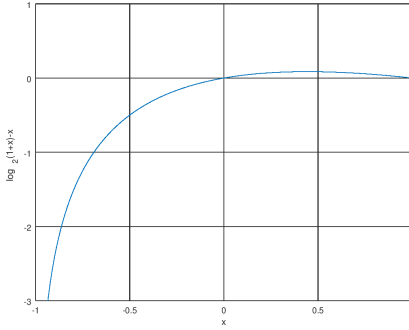
 3: $cut_values \leftarrow [(codebook[i] + codebook[i + 1])/2 \text{ for } i = 0 \text{ to } len(codebook) - 1]$
Output: $codebook, cut_values$


Figure 5. Error in first-order Taylor series expansion of $\log_2(1 + x)$, expanded around zero, for $-1 < x < 1$

operands have opposite signs. Some of the addends will have opposite signs, due to negative-signed weights.

We return to the linear amplitude space (before the accumulation) and map back to the log amplitude space using two small singly-indexed arrays. The first table gives us the mapping from

$$i_x = v_x \pmod{N_{q;a}}$$

to⁷

$$T_q(i_x) = 2^{i_x/N_{q;a}}$$

As long as $N_{q;a}$ is a power of 2, the modulo operation is done by simply bit masking the v_x with $N_{q;a} - 1$, so this translation back to linear amplitude is simply the bit mask and a table look up. From this looked-up value, we can get the actual linear value of the weighted unit input as

$$s_x \text{bitshift}(T_q(i_x), o_x)$$

where $o_x = \lfloor \frac{v_x}{N_{q;a}} \rfloor$ and s_x is the sign bit for x . Similar to the modulo operation, we can determine o_x using a simple

⁷The actual values that are returned from $T_q(i_x)$ are scaled up by $N_{o;a} + 3$ (as described below), to allow us to use integer arithmetic but, for ease and clarity of discussion, we don't include that power-of-two scaling for the fixed point computation in this portion.

shifting operation (without division), as long as $N_{q;a}$ is a power of two.

The values for the weighted inputs to the unit are then added together in linear space, using a fixed-point accumulator. The fixed-point scale should be $2^{(N_{o;a}+3)}/S_{max}$ where $S_{max} = 2^{\lceil \log_2 \max(a) \rceil}$ is the next power of two larger than the maximum amplitude of the activation quantizations and $S_{max}2^{-(N_{o;a}+1)}$ is just below the minimum amplitude of the activation quantizations. The additional 2 bits of precision will allow us to return to the log-amplitude space with full resolution of even the lowest octave samples.

If we find that we need to keep precision for the lowest octave when adding and subtracting entries from the highest octave, we can ensure that $T_q()$ (the log-amplitude-to-linear-amplitude table) has entries with at least $N_{o;a} + 3$ bits. The accumulator itself will need to have additional ‘‘head room’’ beyond these $(N_{o;a} + 3)$ bits, to avoid underflow and overflow. Additionally, we can reduce that expected dynamic range that the accumulator needs to handle using our training examples to determine the lowest–maximum-variance order in which to add together the weighted inputs.

Having accumulated all of the weighted inputs, we need to return to the log-amplitude domain using a linear-to-log-amplitude table, $T_q^{-1}()$. To do this reverse mapping:

1. We note the sign of the accumulated value and use that sign as our new s_x .
2. We determine the octave of the result, o_x , by counting the number of leading zeros in our accumulator and adjusting for S_{max} and for the accumulator head room. This leading-zeros count can be done efficiently, without conditional logic, using the approach named ‘‘nlz10a()’’ in (Warren, 2013).
3. We use the $N_{o;a} + 2$ bits just below the leading non-zero (lopping off the leading 1) as our index into the linear-

to-log-amplitude table $T_q^{-1}(v) = \log_2(2^{v/(4*N_{q;a})})$.

The final accumulator-output in log representation will have the sign s_x (from step 1) and the value $-o_x + T_q^{-1}(v_x)$ (from steps 2 and 3). Using $4N_{q;a}$ entries in this reverse-mapping table allows us to distinguish the values at the low end of the octave.

In summary, we have demonstrated how to eliminate all multiplications by moving to log-amplitude quantization. We have found that this representation is well suited for weights. For representing activations, empirically, it does not fit as well in the networks we have tried. For example, with AlexNet, we needed more quantization levels when using octave-based sampling on the activations than we needed using simple linear sampling. Upon further analysis, we noted that to achieve the same level of performance we needed to ensure that the largest step size between activation levels was no bigger than the step size for the linearly spaced activation levels to which we are comparing.